Tumorigenic Conversion of Primary Human Esophageal Epithelial Cells Using Oncogene Combinations in the Absence of Exogenous Ras

Seok-Hyun Kim,[1] Hiroshi Nakagawa,[2] Arunasalam Navaraj,[1] Yoshio Naomoto,[4] Andres J.P. Klein-Szanto,[3] Anil K. Rustgi,[2] and Wafik S. El-Deiry[1]

[1]Laboratory of Molecular Oncology and Cell Cycle Regulation, Departments of Medicine (Hematology/Oncology), Genetics, Pharmacology, the Institute for Translational Medicine and Therapeutics and the Abramson Comprehensive Cancer Center, University of Pennsylvania School of Medicine; [2]Departments of Medicine (Gastroenterology), Genetics, and the Abramson Comprehensive Cancer Center; [3]Medical Science Division, Fox Chase Cancer Center, Philadelphia, Pennsylvania; and [4]Department of Gastroenterological Surgery, Transplant, and Surgical Oncology, Graduate School of Medicine and Dentistry, Okayama University, Okayama, Japan

Abstract

To investigate pathways of human esophageal squamous cell transformation, we generated esophageal tumor cells using human telomerase– and SV40-immortalized primary esophageal epithelial cells (EPC2) by overexpression of selected combinations of oncogenes. H-Ras, c-Myc, or Akt, but not epidermal growth factor receptor (EGFR), induced transformed colonies in soft agar. By contrast, bioluminescence imaging of genetically altered immortalized esophageal cells revealed that Akt, EGFR, or H-Ras, but not c-Myc, resulted in tumor formation in immunodeficient mice. H-Ras-driven tumors showed highly tumorigenic phenotypes with 2.6 ± 0.6 days for doubling, whereas Akt and EGFR tumors doubled every 9.5 ± 1.6 and 6.1 ± 1.2 days, respectively. H-Ras-driven tumors expressed the hypoxia-inducible factor target Glut1, whereas Akt- or EGFR-driven tumors had evidence of angiogenesis and no detectable Glut1 expression. Proliferation rates among these tumors were similar, but there was reduced apoptosis in the more aggressive H-Ras-driven tumors that also developed aneuploidy and multiple centrosomes. c-Myc overexpression did not result in tumorigenic conversion but introduction of Bcl-XL into c-Myc-expressing cells generated tumors. Although cytokeratin expression was typical of squamous carcinoma, gene expression profiling was done to compare the four different types of engineered tumors with human esophageal squamous cell carcinomas and adenocarcinomas. Interestingly, c-Myc plus Bcl-XL transformants mimicked squamous carcinomas, whereas H-Ras-, EGFR-, and Akt-driven tumors were similar to adenocarcinomas in their molecular profiles. These genetically engineered models may provide new platforms for understanding human esophagus cancer and may assist in the evaluation of new therapies. (Cancer Res 2006; 66(21): 10415-24)

Introduction

Generation of human tumor cell lines and xenografts provides a valuable tool for understanding malignant transformation. Because the discovery that Myc and Ras oncogenes together could transform primary mouse embryo fibroblasts (1), many transformed rodent cells have been used as model systems. Although primary human cells have proven to be more resistant to oncogenic challenge (2, 3) in part due to undetectable telomerase activity in most primary cells (4, 5), recent efforts have successfully generated human tumor cell lines from primary cells, including fibroblasts, glial, mammary epithelial cells, and airway epithelial cells (1, 6–11). The SV40 early region (*SV40ER*), human telomerase (*hTERT*), and mutant *Ras* genes were used to transform the human cells. It has also been possible to generate human transformed cells without exogenous telomerase activity (11). Interestingly, in the previous reports, mutant Ras was used widely in all gene combinations to generate the human tumor cell lines.

Carcinogenesis is a multistep process that in part requires inactivation of cellular tumor suppressor genes as well as activation of various oncogenes (12–14). This process is usually tissue specific and the profile of genes activated or inactivated reflects this diversity. For esophageal squamous carcinoma, there are few cases of Ras mutation that have been reported (15–17). Frequent genetic changes associated with the development of esophageal cancer include p53 mutation, inactivation of p16, cyclin D1 amplification, c-Myc or epidermal growth factor (EGF) receptor (EGFR) overexpression (18).

We immortalized human primary esophageal epithelial cells by introducing the *SV40ER* and *hTERT* genes (19, 20). We further tested the transforming and tumorigenic potential of the cells after transfer of several oncogenes relevant to esophageal squamous carcinogenesis, including c-Myc, a constitutively active form of Akt, wild-type (WT) EGFR, or mutant H-Ras. We found that Akt, WT EGFR, or activated H-Ras transfer could lead to the tumorigenic conversion of immortalized primary human esophageal epithelial cells, whereas c-Myc required the addition of Bcl-XL expression to form tumors. Further analysis of the histology of these tumors, their cytokeratin expression, and their gene expression profiles were done and compared with human esophageal squamous cancers and adenocarcinomas. Whereas c-Myc plus Bcl-XL–driven tumors were similar to human squamous cell carcinomas, the Akt-, EGFR- or activated H-Ras-driven tumors appeared more similar to human adenocarcinomas of the esophagus in their molecular profiles. Further insights into the kinetics of tumor growth emerged from analysis of blood vessel formation, expression of the hypoxia-inducible factor (HIF) target Glut1 as a marker for

Note: Supplementary data for this article are available at Cancer Research Online (http://cancerres.aacrjournals.org/).

This work was presented at the 95th Annual Meeting of the AACR in Orlando, Florida (2004).

Requests for reprints: Wafik S. El-Deiry, Department of Medicine (Hematology/Oncology), University of Pennsylvania School of Medicine, 415 Curie Boulevard, Clinical Research Building 437, Philadelphia, PA 19104. Phone: 215-898-9015; Fax: 215-573-9139; E-mail: wafik@mail.med.upenn.edu.

doi:10.1158/0008-5472.CAN-06-2104

hypoxia, as well as analysis of proliferation and apoptosis rates within the artificial tumors. The most rapidly growing tumors driven by activated H-Ras expressed the highest levels of Glut1 but harbored fewer apoptotic cells compared with either Akt- or EGFR-driven tumors that had more blood vessel formation and no detectable expression of Glut1. The new oncogene-specific esophagus cancer models may be useful in further understanding differences between human esophagus squamous cell cancer and adenocarcinoma and may be useful in testing of novel therapeutics.

Materials and Methods

Generation of transformed human esophageal epithelial cells. Primary human esophageal epithelial cells (EPC2) were described previously (19). The retroviral expression constructs, pBabe-Zeo-SV40ER, pBabe-Hygro-hTERT, and pBABE-puro-ras-V12 were kindly provided by Dr. Robert Weinberg (Whitehead Institute for Biomedical Research, Cambridge, MA). pFB-neo-EGFR expresses WT human EGFR and was described previously (19). We subcloned the c-Myc cDNA into pLNCX2 (Clontech, Mountain View, CA) to generate pLNC-Myc. The firefly luciferase cDNA was subcloned into pBabe-puro and pKS-neo. The Bcl-XL cDNA was subcloned into pBabe-Bla, which was generated by substitution of the puromycin resistance gene within pBabe-puro by the blasticidine resistance gene from pcDNA6 (Invitrogen, Carlsbad, CA). Amphotrophic retroviruses were generated from Phoenix-Ampho cells by transfection using LipofectAMINE Plus (Invitrogen) according to the manufacturer's instruction. The viral supernatants were used to infect EPC2 cells using the spinoculation method (21, 22) to decrease the serum exposure time of EPC2 cells to prevent serum-induced differentiation. Retroviruses were introduced serially and drug selection was done to generate pooled clones. Cells were selected in the following concentrations of drugs: 100 μg/mL zeocin, 3 μg/mL hygromycin, 1 μg/mL puromycin, 400 μg/mL G418, or 3 μg/mL blasticidine. After SV40ER and hTERT introduction into EPC2 cells (T-Te), these cells were cultivated in 1:1 mixture of keratinocyte serum-free medium (KSFM), which contains bovine pituitary extract (40 μg/mL), EGF (1 ng/mL), and DMEM with 10% fetal bovine serum (FBS).

Telomeric repeat amplification protocol assay. Cellular extracts were assayed for telomerase activity with a PCR-based telomeric repeat amplification protocol (TRAP) assay (23) using the TRAPeze telomerase detection kit (Chemicon, Temecula, CA). Amplified products were resolved by electrophoresis using 10% nondenaturing polyacrylamide gels. Gels were silver stained to visualize amplified fragments.

***In vivo* bioluminescence imaging of xenografted tumors.** Immunodeficient mice (BALB/c nude, The Jackson Laboratory, Bar Harbor, ME) were maintained under pathogen-free conditions. Cells were suspended in 50% Matrigel and injected s.c. into three or four sites per mouse. Cells (2.5 million) were used per injection. A total of three mice were used for each cell line. Tumor growth was monitored using the Xenogen *In vivo* Imaging System (Xenogen, Alameda, CA). Mice were subjected to imaging within 15 to 30 minutes after i.p. injection of D-luciferin (5 mg/mouse) under anesthesia with i.p. ketamine/xylazine.

Immunohistochemistry. Paraffin sections were dewaxed using xylene and hydrated using a series of ethanol. Microwave antigen retrieval was done using 10 mmol/L citric acid buffer (pH 6) for 15 minutes. Endogenous peroxidases were quenched with 2% hydrogen peroxide, endogenous biotin blocked with an avidin/biotin blocking kit (Vector Laboratories, Burlingame, CA), and followed by protein blocking using Protein Blocking Agent (Coulter Immunotech, Marseille, France). Sections were incubated overnight with primary antibodies, washed the next day with PBS, incubated with biotinylated secondary antibodies (Vector Laboratories), incubated with Vecta Elite avidin-biotin complex method kit (Vector Laboratories), developed with a 3,3′-diaminobenzidine kit (Vector Laboratories), and counterstained with hematoxylin. Specimens were imaged on a Nikon (Melville, NY) E600 Eclipse microscope and equipped with a CoolSnap CCD camera (Roper Scientific, Tucson, AZ).

Primary antibodies included mouse anti-cytokeratin 4 (1:150; Novocastra, Newcastle, United Kingdom), mouse anti-cytokeratin 5 (1:1,000; Novocastra), mouse anti-p53 (1:500; Novocastra), rabbit anti-SV40 (1: 500; Santa Cruz Biotechnology, Santa Cruz, CA), and rabbit anti-Glut1 (1:750; Chemicon).

Karyotyping of chromosomes. Fresh medium containing colcemid (0.02 μg/mL; Sigma, St. Louis, MO) was added to exponentially growing cells. Cells were incubated for a minimum of 1 hour at 37°C, trypsinized, and spun down at low speed. The cell pellet was suspended in 5 mL of 0.56% KCl solution for 6 minutes at room temperature. After brief centrifugation, the pellet was suspended in 5 mL methanol/acetic acid (3:1) fixative and incubated for 5 minutes at room temperature. This step was repeated thrice and cells were suspended in 1 mL fixative solution. This cell suspension was dropped from 2 feet height onto ice-cold glass slides and air dried. The slides were stained with the Giemsa stain at 1:20 dilution overnight (Sigma) and visualized under light microscopy.

Centrosome staining. Cells were seeded in four chamber slides (0.5 million per chamber) and grown overnight. Cells were fixed in methanol/acetone (1:1) for 20 minutes at −20°C and rehydrated with PBS. Cells were permeabilized with 0.5% Triton X-100 in PBS for 5 minutes on ice followed by primary antibody (1:1,000 dilution) incubation at room temperature overnight in PBS containing 4% goat serum (γ-tubulin, Sigma). Cells were washed with PBS thrice and incubated with secondary antibody conjugated with the Cy-3 fluorochrome for 1 hour at room temperature at a 1:500 dilution. Cells were washed with PBS thrice, stained with 4′,6-diamidino-2-phenylindole, and viewed under fluorescence microscopy.

Microarray analysis. Total RNA was extracted from frozen tissues of eight human esophageal carcinomas and four artificial tumors using the RNeasy mini kit (Qiagen, Valencia, CA). Complementary DNA was synthesized from total RNA using a dT primer tagged with a T7 promoter. Complementary RNA was synthesized by transcription *in vitro* and labeled with biotinylated nucleotides (Enzo Biochem, Farmingdale, NY). All hybridizations were done using the HG-133Av2 GeneChip (Affymetrix, Santa Clara, CA). The raw data were normalized by guanine cytosine–robust multiarray analysis methods (24). Significance analysis of microarrays (SAM)[5] version 2.0 was applied to four squamous and four adenocarcinoma array data sets and 5,764 differentially expressed genes were identified with 9.73% false discovery rate. All the other analyses were done using GeneSpring version 7.2. The gene lists obtained from SAM analysis were filtered by minimum 2-fold change, which resulted in the creation of squamous and adenocarcinoma-specific gene signatures (338 and 377 genes, respectively; total of 715 genes). All 12 samples (4 adenocarcinoma, 4 squamous carcinoma, and 4 artificial tumors) were clustered and a sample tree was generated. Gene lists for signal transduction pathways, apoptosis-related genes, and oncogenes were obtained from the Gene Ontology Consortium[6] and filtered against 715 genes in the carcinoma-specific gene signatures. Principal component analysis was done to evaluate relationships between different tumor samples.

Results

Immortalization of primary human esophageal epithelial cells (T-Te cells). To investigate the transformation of human esophageal epithelial cells, we introduced the SV40ER and the catalytic subunit of the *hTERT* gene sequentially into primary human esophageal epithelial cells (EPC2; refs. 19, 25) using retroviral-mediated gene transfer. After selection with zeocin and hygromycin, SV40 large T-antigen and hTERT gene expression was confirmed by Western blotting and the TRAP assay, respectively (Fig. 1*A* and *B*). The "T-Te" cells grew to >50 passages and were maintained for >1 year without any evidence of senescence. Thus, introduction of the *SV40ER* and the *hTERT* genes immortalized EPC2 cells (19).

[5] http://www-stat.stanford.edu/~tibs/SAM/.
[6] http://www.geneontology.org/.

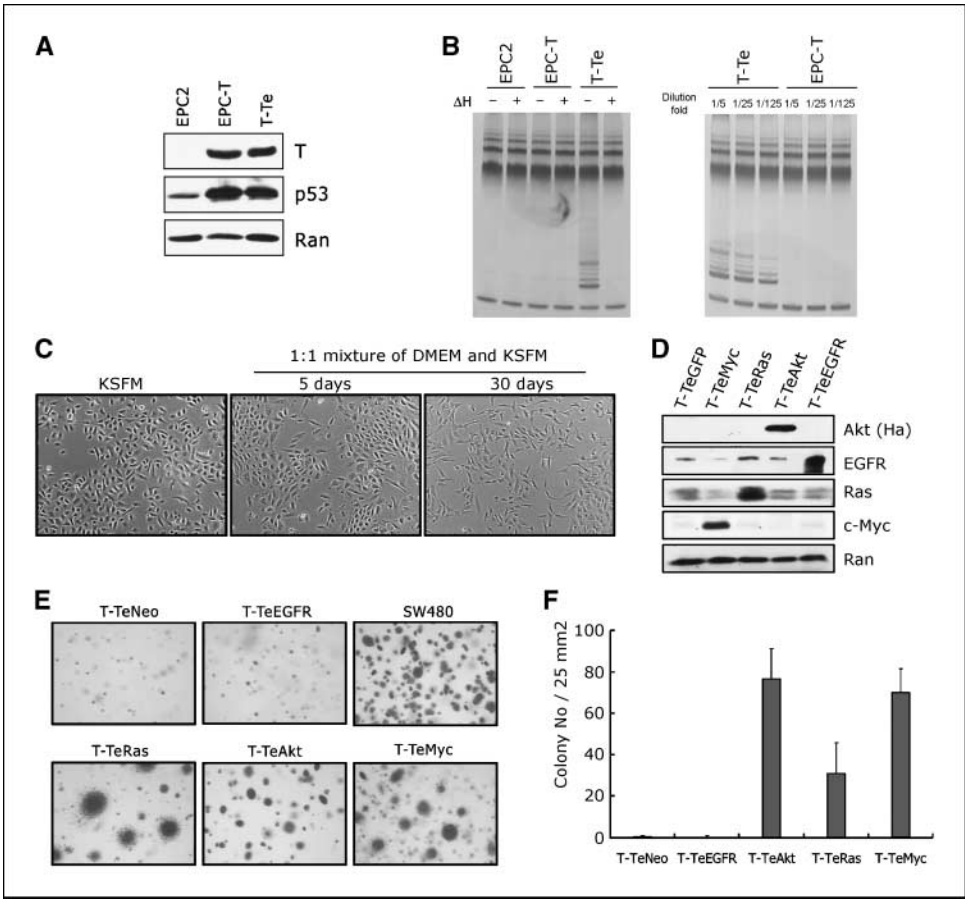

Figure 1. Generation of transformed primary human esophageal cells. *A* and *B,* primary human esophageal epithelial cells (EPC2) were transduced by retroviruses that express the SV40ER and hTERT to generate "T-Te" cells. The activity of SV40 large T antigen was evaluated by checking for p53 protein stabilization. Telomerase activity was confirmed by the TRAP assay. *C,* immortalized esophageal epithelial cells became insensitive to serum-induced differentiation. T-Te cells were exposed to 5% serum-containing medium (1:1 mixture of DMEM with 10% FBS and KSFM). Cells were maintained, subcultured regularly, and showed no sign of cellular growth retardation or senescence. *D,* Akt-, EGFR-, H-Ras-, c-Myc-, or GFP/Neo-expressing retroviruses were infected into T-Te cells. After selection with 1 μg/mL puromycin (Akt, H-Ras, and GFP) or 400 μg/mL G418 (EGFR, c-Myc, and Neo), cells were harvested and subjected to SDS-PAGE and Western blotting to verify expression of oncogenes. *E,* cells (1×10^5) were plated in 6-cm plates containing soft agar and colony growth was measured 2 weeks later. *F,* colonies were counted if the size was >0.2 mm in diameter. The total number of colonies in a 25 mm^2 area was counted and this was repeated five times for each transformant.

Human keratinocytes require a defined culture environment, which could be influenced by serum or calcium to induce differentiation (26). EPC2 cells are primary human keratinocytes and are grown in KSFM, which contains 1 μg/mL recombinant EGF and 40 μg/mL bovine pituitary extract. After immortalization of EPC2, we checked whether this serum-induced differentiation process was still intact because immortalization and transformation processes may be associated with dedifferentiation. When T-Te cells were exposed to 5% serum-containing medium, they appeared well adapted and showed no sign of cell death, senescence, or differentiation (Fig. 1*C*). We therefore cultured T-Te cells in 5% serum-containing medium for the remaining experiments.

Oncogenic stimuli, including Akt, c-Myc, or H-Ras but not EGFR overexpression, transformed T-Te cells *in vitro*. We introduced several oncogenes into T-Te cells and tested the transformation potential of each oncogene using soft agar assays. We chose constitutively active Akt, c-Myc, H-Ras, or EGFR as oncogenes because of their known ability to transform cells as well as their potential involvement in human esophageal squamous cell cancer. Retroviruses containing each oncogene were generated and used to infect T-Te cells, which were then selected with either puromycin (H-Ras, Akt, or GFP) or G418 (EGFR, c-Myc, or neo control). Overexpression of the protein encoded by each exogenous oncogene was verified by Western blotting (Fig. 1*D*). Akt, c-Myc, or H-Ras expression in T-Te cells resulted in a significant morphologic change in culture (data not shown) and also alterations in growth rate. T-Te cells with c-Myc or Akt (T-TeMyc or T-TeAkt) grew much faster than T-TeNeo, whereas cells with the H-Ras oncogene (T-TeRas) displayed a decreased growth rate and the cells with EGFR overexpression (T-TeEGFR) showed no change in cell morphology and also displayed an identical growth rate as the T-TeNeo cells (Supplementary Fig. S1). We found that the Akt, c-Myc, or H-Ras oncogenes, but not EGFR, led to anchorage-independent growth in soft agar of the respective T-Te cells (Fig. 1*E*). T-TeAkt cells formed a large number of compact colonies similar to SW480 human colon cancer cells, which were used as a positive control. T-TeMyc cells formed a large number of colonies in soft agar similar to T-TeAkt cells but the colonies appeared to be less compact. T-TeRas cells grew as much bigger but less compact colonies and were fewer in number compared with either T-TeAkt or T-TeMyc. Although T-TeRas displayed a lower growth rate than T-TeNeo cells in culture (Fig. 1*F*), these cells formed large colonies in soft agar, whereas T-TeNeo and T-TeEGFR did not.

***In vivo* tumor formation following H-Ras, EGFR, or Akt but not c-Myc expression in immortalized T-Te cells.** To correlate *in vivo* tumorigenecity with the *in vitro* and soft agar growth, each cell line was also injected into immunodeficient mice. To facilitate detection of tumor masses formed in the immunodeficient mice, the firefly luciferase gene was introduced into each cell line to monitor bioluminescence as a quantifiable measure of tumor growth. On the day of injection (T-TeRas) or 3 days after injection (T-TeNeo, T-TeAkt, T-TeEGFR, and T-TeMyc), we detected strong luciferase activity but the signal decreased rapidly during first 2 weeks after injection in all groups. The luciferase signal began to increase after 3 weeks but the pattern of increase was different in each group (Fig. 2; Supplementary Movie). Because the injected and

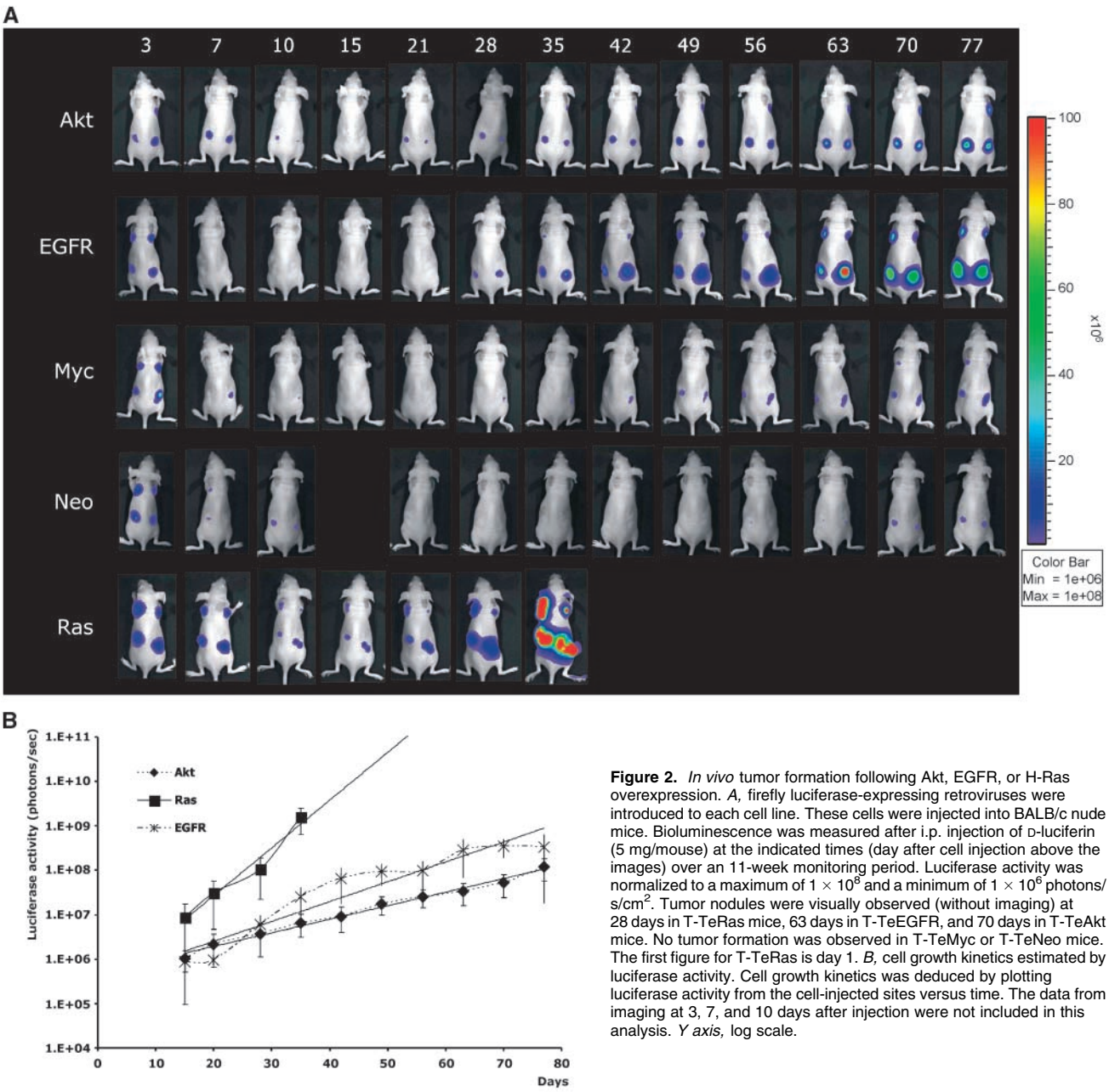

Figure 2. *In vivo* tumor formation following Akt, EGFR, or H-Ras overexpression. *A,* firefly luciferase-expressing retroviruses were introduced to each cell line. These cells were injected into BALB/c nude mice. Bioluminescence was measured after i.p. injection of D-luciferin (5 mg/mouse) at the indicated times (day after cell injection above the images) over an 11-week monitoring period. Luciferase activity was normalized to a maximum of 1×10^8 and a minimum of 1×10^6 photons/s/cm^2. Tumor nodules were visually observed (without imaging) at 28 days in T-TeRas mice, 63 days in T-TeEGFR, and 70 days in T-TeAkt mice. No tumor formation was observed in T-TeMyc or T-TeNeo mice. The first figure for T-TeRas is day 1. *B,* cell growth kinetics estimated by luciferase activity. Cell growth kinetics was deduced by plotting luciferase activity from the cell-injected sites versus time. The data from imaging at 3, 7, and 10 days after injection were not included in this analysis. *Y axis,* log scale.

viable cells were the only source of luciferase activity in the mouse, we could trace cell growth kinetics even before formation of a visible or palpable tumor mass. The most rapidly growing tumor resulted following injection of T-TeRas cells. Small tumor nodules were identified at 28 days and 7 tumor masses with high luciferase signal (>1×10^9 photons/s) were formed by 35 days from 12 independent injections (Table 1). The average doubling time of the T-TeRas tumors was 2.6 ± 0.6 days. In case of EGFR and Akt tumors, we detected an increase in the luciferase signal from the implanted cells after 3 weeks and identified small tumor nodules by 9 weeks (T-TeEGFR) or 10 weeks (T-TeAkt) after injection. The doubling time of T-TeEGFR or T-TeAkt was 6.1 ± 1.2 or 9.5 ± 1.6 days, respectively. Interestingly, T-TeEGFR cells formed growing tumor masses *in vivo* and the tumor-forming ability was even greater than T-TeAkt, although T-TeEGFR cells failed to form colonies in soft agar. In mice that received T-TeMyc injections, we detected no tumor nodules during the 11-week observation period.

Histologic and molecular characteristics of isolated artificial human tumor xenografts. Isolated tumors were composed of poorly differentiated cells and were relatively well circumscribed from the surrounding tissue. All tumor tissues showed strong nuclear staining for SV40 large T antigen and stabilization of p53 protein, confirming that these tumors originated from the implanted cells (Fig. 3*A*). We observed capillary formation in tumor tissues and found that Akt and EGFR tumors, which grew

Table 1. Summary of tumor formation using different T-Te transformants injected into mice

	No. tumor masses/injections
Neo	0/12
Akt	3/11
EGFR	4/12
Myc	0/12
Ras	7/12

slowly, formed many capillaries with strong Lectin BS-6 staining. In contrast, the H-Ras tumor, which grew rapidly, showed numerous Lectin BS-6 staining endothelial cells, but it was difficult to identify vessel structures with a lumen. Concomitantly, we found evidence for focal hypoxic areas within the H-Ras tumor as verified by staining for the human glucose transporter Glut1, which is a transcriptional target of the HIF (Fig. 3*B*). When we analyzed cell proliferation and apoptosis in the tumors, active proliferation and concomitant apoptosis were observed in Akt- and EGFR-overexpressing tumors, whereas the mutant Ras-overexpressing tumor showed active proliferation but very low levels of apoptosis (Fig. 3*C*). Thus, we speculate the major difference in tumor growth kinetics might have originated from the differences in apoptosis rather than proliferation within the tumors.

We further analyzed these tumors, derived by transformation of primary esophageal epithelial cells, to determine if they expressed cytokeratin 4 and 5 expression patterns characteristic of human esophageal cancer. Human esophageal squamous carcinomas typically stain with cytokeratin 5 but less with cytokeratin 4, which shows very weak staining, whereas adenocarcinomas show strong cytokeratin 4 staining but weak or absent cytokeratin 5 (Fig. 3*D*; refs. 27–29). Staining of tumor xenografts showed focally positive cytokeratin 5 expression and negative cytokeratin 4 protein expression (Fig. 3*E*).

Bcl-XL expression was required for c-Myc to form tumors when expressed in T-Te cells. c-Myc expression has been detected

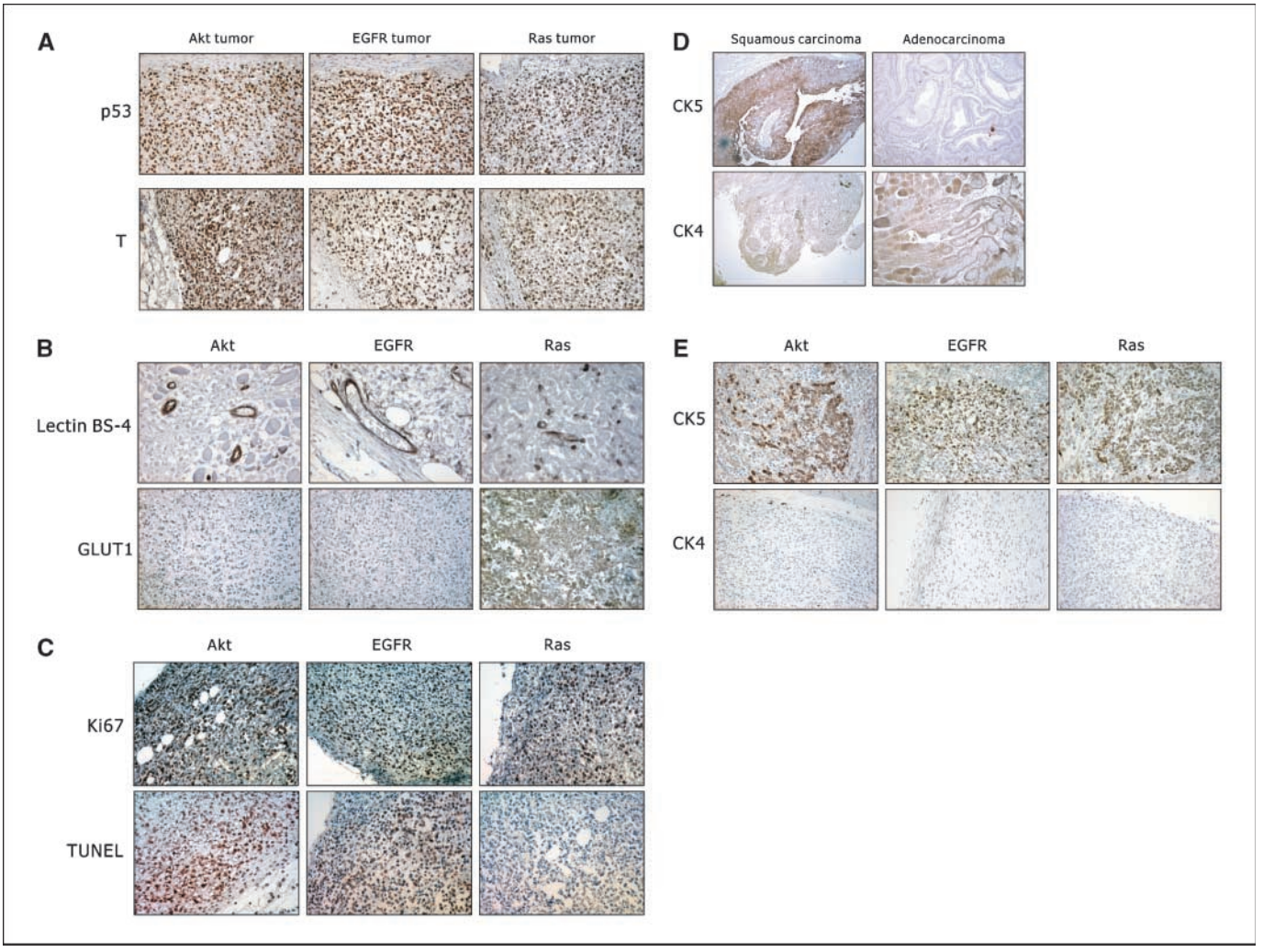

Figure 3. Histologic and molecular characteristics of isolated artificial human tumor xenografts. *A,* tumor sections were stained with SV40 large T antigen and human p53 to verify the tumors originated from the cells that were injected. *B,* lectin staining was carried out to visualize vascular structures. Akt- or EGFR-overexpressing tumors showed numerous vessel structures, whereas mutant Ras-overexpressing tumors showed poor and distorted vasculature, which correlated with focal hypoxic areas detected by human glucose transporter 1 protein staining. *C,* cell proliferation and apoptosis were examined in the tumors by Ki67 staining and terminal deoxynucleotidyl transferase–mediated dUTP nick end labeling assay (*TUNEL*). *D,* cytokeratin expression in human esophageal squamous carcinoma and adenocarcinoma. *E,* cytokeratin staining in artificial tumors. Staining for cytokeratins 4 and 5 is shown.

in advanced esophageal cancers and its expression is correlated with poor prognosis (30). Myc is a potent oncogene but is also an inducer of apoptosis. It is generally believed that, for c-Myc to act as an oncogene, inhibition of apoptosis must occur due to other gene alterations, such as up-regulated expression of Bcl2 or Bcl-XL. To test this prediction, we introduced the *Bcl-XL* gene into T-Te or T-TeMyc cells (Fig. 4*A*) and tested for tumor formation in nude mice. T-TeMyc-Bcl-XL cells formed tumors in three of five mice, whereas T-TeBcl-XL cells did not form any tumors (Fig. 4*B*). Myc-Bcl-XL tumors were palpable nodules within 3 weeks after injection that is earlier than the time required for Akt or EGFR to form tumors. However, the Myc-Bcl-XL-driven tumors grew more slowly compared with the activated H-Ras-driven tumors (data not shown). The cytokeratin expression pattern of Myc-Bcl-XL tumors was similar to those of other tumors (Fig. 4*C*).

Aneuploidy was observed in the highly malignant H-Ras tumors. Although four types of tumors were generated using distinct combinations of oncogenes, the H-Ras tumors were the only ones that displayed a highly malignant phenotype. Even the Myc-Bcl-XL combination, which grew tumor nodules by 3 weeks after injection, did not grow as fast as the activated H-Ras-driven tumors. Analysis for aneuploidy within the cells used to inject mice (T-TeNeo, Akt, EGFR, Myc, Ras, Bcl-XL, and Myc-Bcl-XL) revealed that T-TeRas were the only ones with a polyploid population of cells and mitomycin C treatment expanded this population, whereas all the other cell lines were not expanded with mitomycin C treatment (Fig. 5*A*). We also found inappropriate centrosome replication that resulted in multiple centrosomes in the nuclei of T-TeRas cells (Fig. 5*B*). Aneuploidy was confirmed by karyotyping. We identified hypodiploid or polyploid chromosomes in metaphase arrested T-TeRas cells (Fig. 5*C*). All the other cell lines, including cells that formed tumors, did not show aneuploidy regardless of treatment with mitomycin C (data not shown). Thus, H-Ras oncogene overexpression led to chromosomal instability and this may be a critical factor for the highly malignant phenotype of the activated H-Ras-driven tumors.

Distinct gene expression profiles within artificial human esophageal cancers. Because the engineered tumor cells appeared to mimic human squamous cancers by cytokeratin staining, we further evaluated global gene expression patterns within these tumors and compared them with human squamous cell carcinomas or adenocarcinomas. Four human esophageal adenocarcinomas and four human esophageal squamous cell carcinomas were used to obtain gene expression profiles and these were compared with profiles from the four engineered tumors (Akt-, EGFR-, activated H-Ras-, and Myc-Bcl-XL-driven tumors). Squamous cell carcinoma–specific and adenocarcinoma-specific gene signatures (338 and 377 genes, respectively) were obtained with a 10% false detection rate and minimal 2-fold change in gene expression. When we applied these gene signatures to our four engineered tumors and did a cluster analysis, we found that Akt-, EGFR-, and activated H-Ras-driven tumors were relatively similar to adenocarcinomas, whereas the Myc-Bcl-XL-driven tumors were similar to the squamous cell carcinomas (Fig. 6*A*). However, principal component analysis showed a wide separation of the engineered tumors from either squamous cell carcinomas or adenocarcinomas (Fig. 6*B*). To further examine the similarities between the engineered tumors and the naturally occurring human tumors, we selected genes from among the carcinoma-specific gene signatures for categorization into functional categories (see microarray analysis in Materials and Methods). First, we searched classic cytologic markers, which were used to discriminate tissue origin or types of cancers. We found that cytokeratins 10 and 5 were specific for the esophageal squamous carcinoma, whereas Mucin 3, Villin 1, and Villin-like genes were identified as the markers for adenocarcinoma (Supplementary Fig. S2A). When we searched the genes related to signal transduction pathways, 10 genes were differentially expressed. Of 10 genes, we found that genes involved in increasing c-Jun NH_2-terminal kinase and nuclear factor-κB activity were squamous carcinoma specific [MALT1 (31), ADORA2B, and MAP3K4 (32)], whereas phospholipase C-ε1 (PLCE1), which mediates Ras/mitogen-activated protein kinase activation (33),

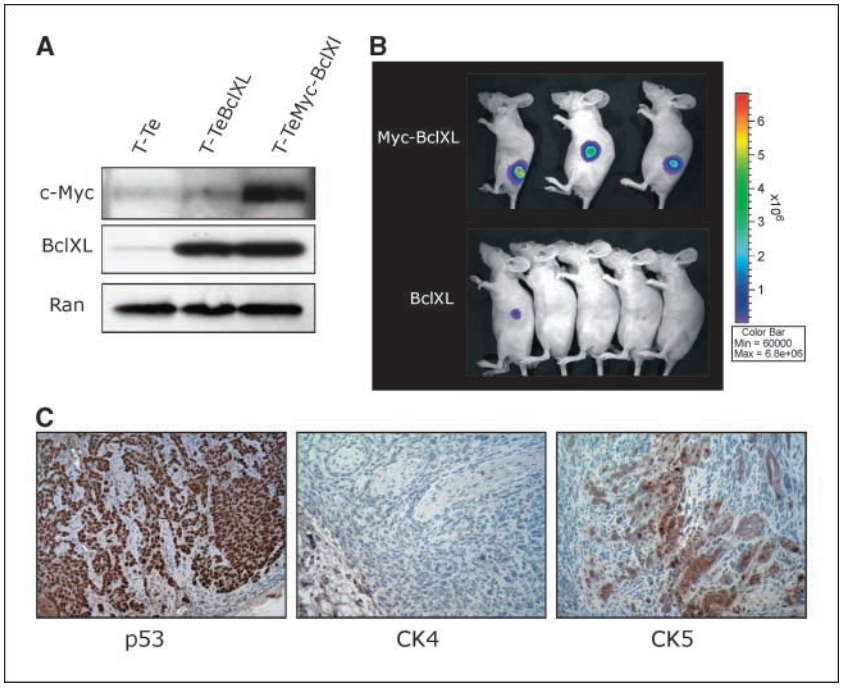

Figure 4. Bcl-XL expression cooperated with c-Myc to form tumors. *A,* Bcl-XL expression was confirmed after introduction of the Bcl-XL cDNA into T-Te and T-TeMyc cells. *B,* T-TeBcl-XL and T-TeMyc-Bcl-XL cells were introduced into nude mice. Bioluminescence images was taken at 7 weeks after injection. T-TeBcl-XL did not form tumors, although some mice showed minimal luciferase activity. T-TeMyc-Bcl-XL cells formed tumors in three of five mice. *C,* sections of Myc-Bcl-XL tumors were stained for p53 as well as cytokeratin 4 and 5 expression.

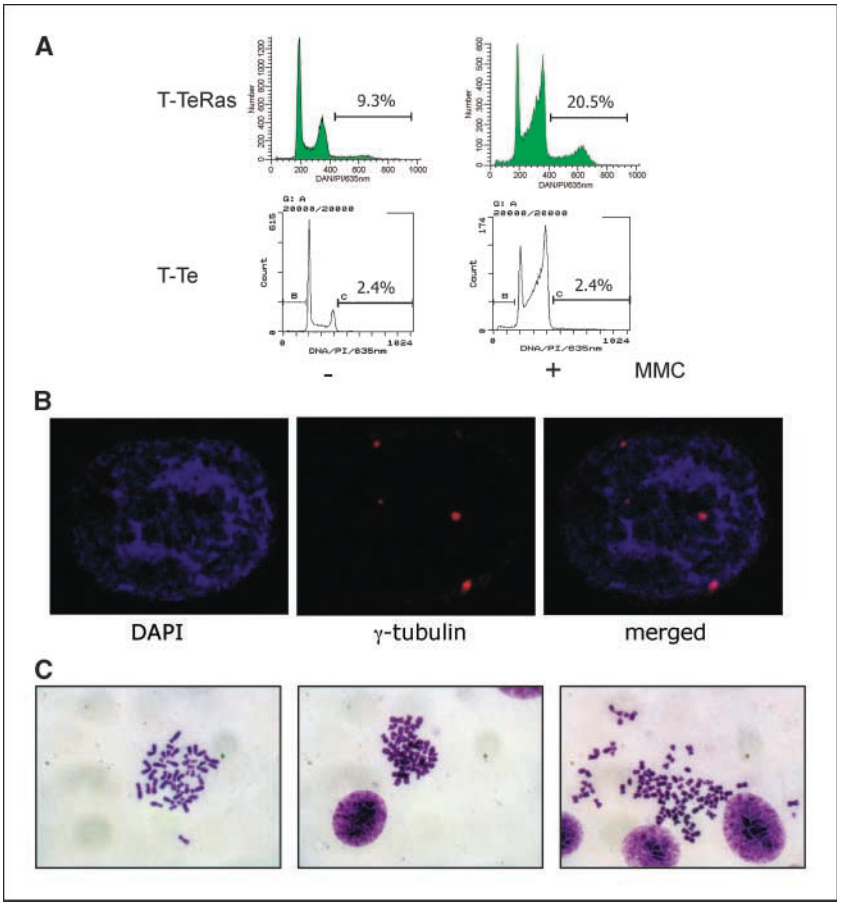

Figure 5. T-TeRas was unique among the artificial tumors in showing an aneuploidy phenotype. *A,* T-TeRas and T-TeNeo cells were subjected to analysis of their hyperdiploid populations. T-TeRas cells showed significant hyperdiploid populations and this was increased by mitomycin C treatment (100 ng/mL for 24 hours). *B,* inappropriate replication of centrosomes. Multiple centrosomes in nuclei after mitomycin C treatment were observed in T-TeRas tumor cells. *C,* chromosome staining of metaphase arrested T-TeRas cells. A diploid cell showed 46 chromosomes (*left*), a hypodiploid cell showed 37 chromosomes (*center*), and a hyperdiploid cell showed 69 chromosomes (*right*).

was adenocarcinoma specific (Supplementary Fig. S2B). We also categorized 16 apoptosis-related genes (Supplementary Fig. S2C) and 20 oncogenes (Supplementary Fig. S2D) and found that TP73L (p63), Bcl2/adenovirus E1B-interacting protein 3 (BNIP3), and Myc expression was increased in squamous carcinoma. In adenocarcinoma, death-associated protein kinase 1 (DAPK1), Bcl2-associated athanogene 1 (BAG1), HER3 (ERBB3) expression was increased. Principal component analysis using these categorized gene lists showed that Myc-Bcl-XL tumors were more similar to squamous cell carcinomas, whereas Akt, EGFR, and H-Ras tumors were more similar to adenocarcinomas.

Discussion

We show that Akt, EGFR, or activated H-Ras can convert human immortalized primary esophageal epithelial cells into tumorigenic cancer cell lines, whereas c-Myc required Bcl-XL expression to form tumors. Although H-Ras was reported previously as an effective oncogene for the transformation of human primary esophageal cells, we believe this is first report that Akt, EGFR, or Myc-Bcl-XL could generate tumors with a background of immortalization by *hTERT* and *SV40* early genes.

EGFR plays an important role in multiple cellular functions, including proliferation, differentiation, and survival (34). Amplification of *EGFR* gene is frequently found in esophageal cancers (35, 36) and activation of EGFR influences phosphatidylinositol 3-kinase (PI3K), Janus-activated kinase/signal transducer and activator of transcription (37), and extracellular signal-regulated kinase 1 (38, 39). EGFR expression is also correlated with tumor angiogenesis (40) and was identified as a candidate mediator of the highly angiogenic nature of childhood astrocytomas by gene profiling (41). There are few reports about Akt involvement in esophageal carcinogenesis but elevated phosphorylation of Ser^{473} of Akt has been observed in esophageal cancer cell lines (42). Akt has been implicated in tumor angiogenesis and metastasis of colon cancers (43). Our results show that Akt- and EGFR-driven tumors have similar growth kinetics in *in vivo* tumor formation and by staining for several histologic markers. We observed vascularization especially at the periphery of these tumors that did not express detectable levels of Glut1, a HIF target and marker of hypoxia. This similarity is consistent with a role for Akt in EGFR signaling in esophageal carcinogenesis. Interestingly, the Akt- or EGFR-driven tumors contained significant populations of cells undergoing apoptosis with other populations undergoing active proliferation. We conclude that apoptosis limited the observed tumor growth in the Akt- or EGFR-driven tumors.

For the c-Myc oncogene, we observed no tumor formation using T-TeMyc cells injected into mice, although c-Myc is an important oncogene in many types of cancer, including esophageal cancer (35, 44). This finding is consistent with other reports, in which c-Myc overexpression could transform cells but not lead to tumor formation (10). c-Myc is an oncogene but also a strong inducer of apoptosis. c-Myc could induce apoptosis in primary cells via the ADP ribosylation factor pathway and, even in transformed cells, c-Myc overexpression is closely related to sensitization of tumor cells to death stimuli, including tumor necrosis factor–related

apoptosis-inducing ligand treatment (45). c-Myc requires additional gene alterations that could block apoptosis in order for c-Myc to exert its oncogenic properties. This was verified by introduction of antiapoptotic gene *Bcl-XL* into T-TeMyc cells that were able to form tumors. This suggests that c-Myc oncogene activation may contribute to tumor formation at a later step in carcinogenesis after the apoptosis function suppressed. We believe this may explain why c-Myc overexpression is found more frequently in advanced cancers (44).

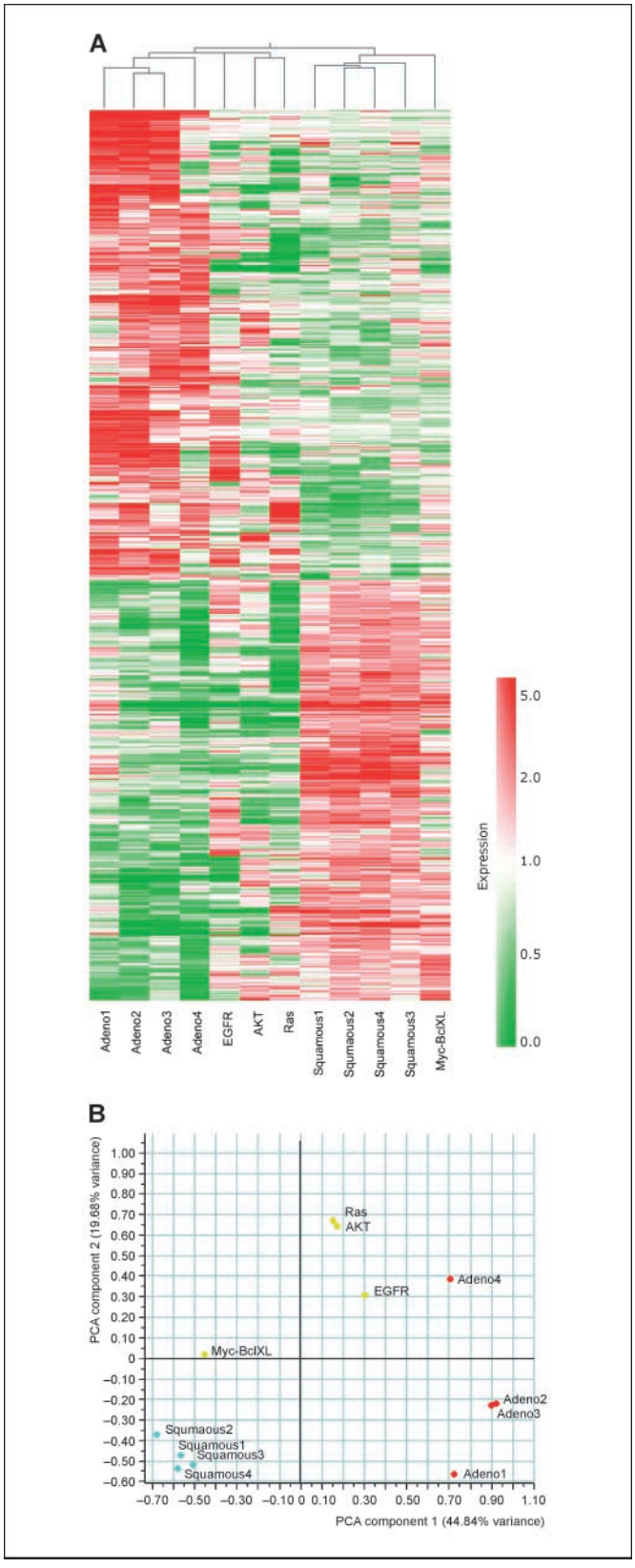

Although it is not a frequently involved oncogene in esophageal carcinogenesis, overexpression of activated H-Ras made cells tumorigenic and tumor masses were generated by 4 weeks after injection. Activated H-Ras-driven tumors displayed a highly malignant phenotype. We could identify focal hypoxic areas and poor vessel formation with abundant endothelial cell staining in the H-Ras-driven tumors. H-Ras overexpression is reported to closely relate to the hypoxic nature of the tumors (46, 47). Downstream pathways of H-Ras are mainly Raf, PI3K, and Ral-GEFs and their individual effect in transformation has been evaluated elsewhere (48). We found that only H-Ras overexpression could generate polyploidy of the chromosomes and centrosome amplification that may have contributed to the transforming ability of the H-Ras gene.

We analyzed the nature of our engineered tumors by comparing their gene expression patterns with human esophageal carcinomas. The results show that the engineered tumors are different from spontaneous human cancers in terms of genetic signatures. This might be explained by two reasons. First, the engineered tumors did not contain the full spectrum of genetic alterations associated with the human tumors. Each tumor had only one or two genetic alterations in a background of immortalization by the *SV40ER* and *hTERT* genes. Further efforts to introduce additional genes and/or gene combinations involved in esophageal carcinogenesis may in the future better match the genetic signatures with either human squamous cell carcinomas or adenocarcinomas of the esophagus. Such experiments may in the future also include modified stromal compartments. Second, using the SV40ER for immortalization of primary cells might have resulted in differences between the artificial tumors and spontaneous human esophageal tumors. The proteins blocked by SV40 large and small T antigens include p53, pRB, HSP70, p300, and PP2A and there may be other unknown targets disrupted by SV40. Avoiding viral oncogenes in generating tumorigenic cell lines from primary human cells is a potential future direction, although our preliminary experience suggests that SV40ER may be a powerful and effective tool and that substitution of multiple endogenous targets may be challenging.

In summary, we have created new mouse models of human esophagus cancer using primary human esophageal epithelial cells that were immortalized and subsequently transformed by various oncogenes, including activated H-Ras, Akt, EGFR, and c-Myc plus Bcl-XL. Noninvasive imaging was used to document kinetics of tumor growth and this revealed a range of aggressive behavior with activated H-Ras at one extreme to Akt at the other in terms of rate of tumor growth *in vivo*. c-Myc alone was not sufficient to form

Figure 6. Comparison of gene expression profiles of artificial tumors and human esophageal squamous carcinomas or adenocarcinomas. *A,* 715 tumor type-specific genes (338 genes for squamous and 377 genes for adenocarcinoma) were used for sample tree generation. Akt, EGFR, and Ras tumors were similar to the adenocarcinomas, whereas the Myc-Bcl-XL tumor was similar to the squamous carcinomas. *B,* principal component analysis using the 715 genes showed some separation of artificial tumors from the human cancer samples. Akt, EGFR, and Ras tumors were relatively similar to the esophageal adenocarcinomas and the Myc-Bcl-XL tumor was similar to the squamous carcinomas of the esophagus.

tumors in mice and required Bcl-XL to inhibit apoptosis. The activated H-Ras-driven tumors, but not the Akt- or EGFR-driven tumors, displayed genomic instability, expression of Glut1 as a marker of hypoxia, and reduced apoptosis. Although it is clear that activated H-Ras was very effective in tumorigenic conversion of immortalized esophageal epithelial cells, an important advance is the demonstration of tumor formation through gene transfer of combinations that did not include activated H-Ras. Another important advance is documentation using oligonucleotide microarrays of gene expression signatures among different tumors and in comparing the genetically engineered tumors with spontaneously occurring human squamous cell carcinomas or adenocarcinomas of the esophagus. Such analyses have seldom been done (e.g., to compare transgenic mouse models with human tumors in part due to technical difficulties in analyzing microarray data cross-species). Interestingly, our c-Myc plus Bcl-XL–driven tumors were more similar to the squamous tumors, whereas the activated H-Ras-, Akt- or EGFR-driven tumors had more similarity to adenocarcinomas of the esophagus in their gene expression profiles. These advances provide a starting point for future studies that can further refine the models and make use of them in better understanding the role of specific oncogenes in esophagus cancer, including the role of activated H-Ras in inducing genomic instability and the specific or consistent genomic alterations, if any, which may be occurring in these specific tumors. Further studies are required to analyze specific molecular changes in signaling that ultimately affect on tumor vascularity and apoptotic rates within the engineered esophageal tumors. In particular, it will be of interest to identify differences between the Akt- or EGFR-driven tumors that had clear evidence of blood vessel formation, no evidence of hypoxia, and more apoptosis compared with the activated H-Ras-driven tumors. In this regard, preliminary analysis of the gene expression patterns among these tumors have revealed decreased expression of interleukin-8 (IL-8) mRNA in EGFR-driven (55-fold) or Akt-driven tumors (93-fold) compared with the activated H-Ras-driven tumors. This is consistent with recent observations linking IL-8 as a transcriptional target of Ras signaling with stromal responses, including inflammation and cancer progression (49). We note that BNIP3 was decreased 44-fold in the Akt-driven tumors compared with the activated H-Ras-driven tumors, consistent with the high Glut1 expression in the H-Ras-driven tumors that likely reflects hypoxia. Despite their increased BNIP3 levels, the activated H-Ras-driven tumors were more resistant to apoptosis likely due to the prosurvival effects of H-Ras (50). Using these models as well as ones using other oncogenes that can be generated using similar approaches, it may be possible in the future to better understand the role of specific oncogenes in therapeutic responses. Such translational preclinical data may be very helpful in clinical trial design for patients with esophagus cancer.

Acknowledgments

Received 6/8/2006; revised 7/27/2006; accepted 8/7/2006.

Grant support: NIH grants CA098101 and CA105008 and excellent core facilities at the University of Pennsylvania School of Medicine.

The costs of publication of this article were defrayed in part by the payment of page charges. This article must therefore be hereby marked *advertisement* in accordance with 18 U.S.C. Section 1734 solely to indicate this fact.

We thank John Tobias for assistance with the analysis of the microarray data.

References

1. Land H, Parada LF, Weinberg RA. Tumorigenic conversion of primary embryo fibroblasts requires at least two cooperating oncogenes. Nature 1983;304:596–602.
2. Serrano M, Lin AW, McCurrach ME, Beach D, Lowe SW. Oncogenic ras provokes premature cell senescence associated with accumulation of p53 and p16INK4a. Cell 1997;88:593–602.
3. O'Brien W, Stenman G, Sager R. Suppression of tumor growth by senescence in virally transformed human fibroblasts. Proc Natl Acad Sci U S A 1986;83:8659–63.
4. Kim NW, Piatyszek MA, Prowse KR, et al. Specific association of human telomerase activity with immortal cells and cancer. Science 1994;266:2011–5.
5. Shay JW, Bacchetti S. A survey of telomerase activity in human cancer. Eur J Cancer 1997;33:787–91.
6. Hahn WC, Counter CM, Lundberg AS, Beijersbergen RL, Brooks MW, Weinberg RA. Creation of human tumour cells with defined genetic elements. Nature 1999;400:464–8.
7. Rich JN, Guo C, McLendon RE, Bigner DD, Wang XF, Counter CM. A genetically tractable model of human glioma formation. Cancer Res 2001;61:3556–60.
8. Lundberg AS, Randell SH, Stewart SA, et al. Immortalization and transformation of primary human airway epithelial cells by gene transfer. Oncogene 2002;21:4577–86.
9. Elenbaas B, Spirio L, Koerner F, et al. Human breast cancer cells generated by oncogenic transformation of primary mammary epithelial cells. Genes Dev 2001;15:50–65.
10. Zhao JJ, Gjoerup OV, Subramanian RR, et al. Human mammary epithelial cell transformation through the activation of phosphatidylinositol 3-kinase. Cancer Cell 2003;3:483–95.
11. Seger YR, Garcia-Cao M, Piccinin S, et al. Transformation of normal human cells in the absence of telomerase activation. Cancer Cell 2002;2:401–13.
12. Paulovich AG, Toczyski DP, Hartwell LH. When checkpoints fail. Cell 1997;88:315–21.
13. Sherr CJ. Cancer cell cycles. Science 1996;274:1672–7.
14. Hanahan D, Weinberg RA. The hallmarks of cancer. Cell 2000;100:57–70.
15. Nishihira T, Hashimoto Y, Katayama M, Mori S, Kuroki T. Molecular and cellular features of esophageal cancer cells. J Cancer Res Clin Oncol 1993;119:441–9.
16. Arber N, Shapira I, Ratan J, et al. Activation of c-K-ras mutations in human gastrointestinal tumors. Gastroenterology 2000;118:1045–50.
17. Jiang W, Kahn SM, Guillem JG, Lu SH, Weinstein IB. Rapid detection of ras oncogenes in human tumors: applications to colon, esophageal, and gastric cancer. Oncogene 1989;4:923–8.
18. Mandard AM, Hainaut P, Hollstein M. Genetic steps in the development of squamous cell carcinoma of the esophagus. Mutat Res 2000;462:335–42.
19. Andl CD, Mizushima T, Nakagawa H, et al. Epidermal growth factor receptor mediates increased cell proliferation, migration, and aggregation in esophageal keratinocytes *in vitro* and *in vivo*. J Biol Chem 2003;278:1824–30.
20. Harada H, Nakagawa H, Oyama K, et al. Telomerase induces immortalization of human esophageal keratinocytes without p16INK4a inactivation. Mol Cancer Res 2003;1:729–38.
21. Bahnson AB, Dunigan JT, Baysal BE, et al. Centrifugal enhancement of retroviral mediated gene transfer. J Virol Methods 1995;54:131–43.
22. Movassagh M, Boyer O, Burland MC, Leclercq V, Klatzmann D, Lemoine FM. Retrovirus-mediated gene transfer into T cells: 95% transduction efficiency without further *in vitro* selection. Hum Gene Ther 2000;11:1189–200.
23. Kim NW, Wu F. Advances in quantification and characterization of telomerase activity by the telomeric repeat amplification protocol (TRAP). Nucleic Acids Res 1997;25:2595–7.
24. Wu Z, Irizarry RA. Preprocessing of oligonucleotide array data. Nat Biotechnol 2004;22:656–8; author reply 658.
25. Kim SH, Kim K, Kwagh JG, et al. Death induction by recombinant native TRAIL and its prevention by a caspase 9 inhibitor in primary human esophageal epithelial cells. J Biol Chem 2004;279:40044–52.
26. Miyashita M, Smith MW, Willey JC, Lechner JF, Trump BF, Harris CC. Effects of serum, transforming growth factor type β, or 12-*O*-tetradecanoyl-phorbol-13-acetate on ionized cytosolic calcium concentration in normal and transformed human bronchial epithelial cells. Cancer Res 1989;49:63–7.
27. Hu YC, Lam KY, Law S, Wong J, Srivastava G. Profiling of differentially expressed cancer-related genes in esophageal squamous cell carcinoma (ESCC) using human cancer cDNA arrays: overexpression of oncogene MET correlates with tumor differentiation in ESCC. Clin Cancer Res 2001;7:3519–25.
28. Suo Z, Holm R, Nesland JM. Squamous cell carcinomas. An immunohistochemical study of cytokeratins and involucrin in primary and metastatic tumours. Histopathology 1993;23:45–54.
29. Taniere P, Martel-Planche G, Maurici D, et al. Molecular and clinical differences between adenocarcinomas of the esophagus and of the gastric cardia. Am J Pathol 2001;158:33–40.
30. Pelengaris S, Khan M, Evan G. c-MYC: more than just a matter of life and death. Nat Rev Cancer 2002;2:764–76.
31. Ruland J, Duncan GS, Wakeham A, Mak TW. Differential requirement for Malt1 in T and B cell antigen receptor signaling. Immunity 2003;19:749–58.
32. Takekawa M, Posas F, Saito H. A human homolog of the yeast Ssk2/Ssk22 MAP kinase kinase kinases, MTK1, mediates stress-induced activation of the p38, and JNK pathways. Embo J 1997;16:4973–82.

33. Lopez I, Mak EC, Ding J, Hamm HE, Lomasney JW. A novel bifunctional phospholipase c that is regulated by Gα 12 and stimulates the Ras/mitogen-activated protein kinase pathway. J Biol Chem 2001; 276:2758–65.
34. Nicholson RI, Gee JM, Harper ME. EGFR and cancer prognosis. Eur J Cancer 2001;37 Suppl 4:S9–15.
35. Lu SH, Hsieh LL, Luo FC, Weinstein IB. Amplification of the EGF receptor and c-myc genes in human esophageal cancers. Int J Cancer 1988;42:502–5.
36. Hollstein MC, Smits AM, Galiana C, et al. Amplification of epidermal growth factor receptor gene but no evidence of ras mutations in primary human esophageal cancers. Cancer Res 1988;48:5119–23.
37. Andl CD, Mizushima T, Oyama K, Bowser M, Nakagawa H, Rustgi AK. EGFR-induced cell migration is mediated predominantly by the JAK-STAT pathway in primary esophageal keratinocytes. Am J Physiol Gastrointest Liver Physiol 2004;287:G1227–37.
38. Sordella R, Bell DW, Haber DA, Settleman J. Gefitinib-sensitizing EGFR mutations in lung cancer activate anti-apoptotic pathways. Science 2004;305:1163–7.
39. Andl CD, Mizushima T, Oyama K, Bowser M, Nakagawa H, Rustgi AK. EGFR induced cell migration is mediated predominantly by the JAK/Stat pathway in primary esophageal keratinocytes. Am J Physiol Gastrointest Liver Physiol 2004;287:G1227–37.
40. Asakuma J, Sumitomo M, Asano T, Asano T, Hayakawa M. Modulation of tumor growth and tumor induced angiogenesis after epidermal growth factor receptor inhibition by ZD1839 in renal cell carcinoma. J Urol 2004;171:897–902.
41. Khatua S, Peterson KM, Brown KM, et al. Overexpression of the EGFR/FKBP12/HIF-2α pathway identified in childhood astrocytomas by angiogenesis gene profiling. Cancer Res 2003;63:1865–70.
42. Okano J, Gaslightwala I, Birnbaum MJ, Rustgi AK, Nakagawa H. Akt/protein kinase B isoforms are differentially regulated by epidermal growth factor stimulation. J Biol Chem 2000;275:30934–42.
43. Agarwal A, Das K, Lerner N, et al. The AKT/IκB kinase pathway promotes angiogenic/metastatic gene expression in colorectal cancer by activating nuclear factor-κB and β-catenin. Oncogene 2005;24:1021–31.
44. Bitzer M, Stahl M, Arjumand J, et al. C-myc gene amplification in different stages of oesophageal squamous cell carcinoma: prognostic value in relation to treatment modality. Anticancer Res 2003;23: 1489–93.
45. Ricci MS, Jin Z, Dews M, et al. Direct repression of FLIP expression by c-myc is a major determinant of TRAIL sensitivity. Mol Cell Biol 2004;24:8541–55.
46. Delmas C, End D, Rochaix P, Favre G, Toulas C, Cohen-Jonathan E. The farnesyltransferase inhibitor R115777 reduces hypoxia and matrix metalloproteinase 2 expression in human glioma xenograft. Clin Cancer Res 2003;9:6062–68.
47. Lim JH, Lee ES, You HJ, Lee JW, Park JW, Chun YS. Ras-dependent induction of HIF-1α785 via the Raf/MEK/ERK pathway: a novel mechanism of Ras-mediated tumor promotion. Oncogene 2004;23:9427–31.
48. Rangarajan A, Hong SJ, Gifford A, Weinberg RA. Species- and cell type-specific requirements for cellular transformation. Cancer Cell 2004;6:171–83.
49. Sparmann A, Bar-Sagi D. Ras-induced interleukin-8 expression plays a critical role in tumor growth and angiogenesis. Cancer Cell 2004;6:447–58.
50. Cox AD, Der CJ. The dark side of Ras: regulation of apoptosis. Oncogene 2003;22:8999–9006.